$Sc_5Ni_2Te_2$: Synthesis, Structure, and Bonding of a Metal−Metal-Bonded Chain Phase, a Relative of Gd_3MnI_3

Paul A. Maggard and John D. Corbett*

Department of Chemistry, Iowa State University, Ames, Iowa 50011

Received September 9, 1998

$Sc_5Ni_2Te_2$ has been prepared by high-temperature solid-state techniques and the structure determined at 23 °C by single crystal and powder X-ray diffraction methods to be orthorhombic, *Pnma* (No. 62) with $Z = 4$, $a = 17.862(1)$ Å, $b = 3.9533(3)$ Å, $c = 10.6398(6)$ Å. The structure contains pairs of eclipsed zigzag chains of nickel atoms that are sheathed by scandium atoms and demarcated from other chains by tellurium atoms. The structure is isotypic with that of $Hf_5Co_{1+x}P_{3-x}$, but shifted atomic positions and a different ordering of the main group and late transition elements give it a clearly 1D character. The differences in dimensionality, ordering, and bonding are discussed, and comparisons are made with Gd_3MnI_3 and rare-earth-metal cluster halides in general.

Introduction

The plethora of new metal-rich chalcogenide phases among the early transition metals have been important for understanding the expression of and interrelationships between metal−metal bonding features among these many compounds. Incorporation of late transition metals has long been known to stabilize both metal-rich halides[1] and chalcogenides that are otherwise unstable with respect to electron count and other binary phases. Recently reported ternary chalcogenides and phosphides of this type include $Ta_9M_2S_6$,[2] $Ta_{11}M_2Se_8$ (M = Fe, Co, Ni),[3] Ta_8NiSe_8 (M = Co, Ni),[4] Hf_8MTe_6 (M = Co, Ni, Ru),[5] $Zr_9M_2P_4$ (M = Co, Ni),[6] $Hf_5Co_{1+x}P_{3-x}$, ($0 < x < 0.5$),[7] Hf_2NiP,[8] and ScNiP.[9]

The study of bonding features in metal-rich chalcogenides of the early transition metals has only recently been extended to group 3 (R) examples, namely, to Sc_2Te[10] and Sc_8Te_3.[11] Their structural and bonding relationships to those of electron-richer analogues allow one to assess the importance of atom sizes, valence electron concentrations, and metal-to-nonmetal proportions in the structure and bonding. The smaller number of metal-based electrons for the earlier transition metals appears to force a reduction in the metal−metal framework dimensionality, as shown in particular for Sc_8Te_3 and Y_8Te_3, relatives of Ti_8Ch_3, Ch = S, Se.[12,13] Stoichiometry and efficient packing apparently dictate that some metal atom pairs may be in close proximity even though theory indicates that there are relatively few or no electrons involved in their bonding, i.e., a classical result of matrix effects.

Metal-rich chalcogenides of scandium and yttrium also show some notable contrasts with parallel structures and stoichiometries of their most reduced halides. The latter are known only with proportionately more nonmetal atoms. Twice as many halogen atoms (X) per chalcogen would be expected for the same electron count per metal atom, and in fact somewhat more ($2 < X/R < 3$) are observed in isolated cluster halides. Condensed chains or tetramers built of recognizable octahedra span a range of $1 < X/R < 2$. The halides structurally serve to sheath the metal cores, in all cases leading to clearer definition of the building blocks. Furthermore, with few exceptions, the known reduced halides are so electron-poor that they also require interstitial heteroatoms ($Sc_2Cl_{12}C$, Y_4I_5C, etc.) which afford central bonding and additional bonding electrons.[14]

In analogy with studies on later transition-metal−chalcogen systems, this article presents the first results of the expansion of this chemistry to ternary systems of scandium, in this case with the incorporation of nickel. The early-late transition metal bonding involved appears to reflect the extra stability of such polar interactions that were first noted by Brewer and Wengert.[15] Mixed-metal features in chalcogenides and phosphides are largely multicapped trigonal prisms of the earlier transition metal centered by a late transition metal. The nonmetals in these generally prefer a similar environment, a tricapped trigonal prism (tetrakaidecahedron). In some ternary phases, the late transition metal and nonmetal (e.g., Co and P, or Ni and S) may exhibit unusual mixed metal/nonmetal occupancies of the same sites, as in ($Hf_5Co_{1+x}P_{3-x}$),[7] evidently because of their similar sizes and site preferences. In the title compound, $Sc_5Ni_2Te_2$, the late-transition metal and the nonmetal have markedly different sizes, and mixed occupancy is not a factor. Furthermore, the relative electron deficiency of the host metal and the larger anion ensure a cooperative reduction in dimensionality of the metal−metal bonded framework as compared with that in $Hf_5Co_{1+x}P_{3-x}$, etc. The new $Sc_5Ni_2Te_2$ is significant in that it represents the extension of early-late transition metal chemistry to ternary chalcogenides of the electron-poorer scandium.

(1) Corbett, J. D. *J. Alloys Compd.* **1995**, *229*, 10.
(2) Harbrecht, B.; Franzen, H. F. *J. Less-Common Met.* **1985**, *113*, 349; Harbrecht, B. *J. Less-Common Met.* **1986**, *124*, 125.
(3) Harbrecht, B. *J. Less-Common Met.* **1988**, *182*, 118.
(4) Conard, M.; Harbrecht, B. *J. Alloys Compd.* **1993**, *197*, 57.
(5) Abdon, R. L.; Hughbanks, T. *Chem. Mater.* **1994**, *6*, 424.
(6) Kleinke, H.; Franzen, H. F. *Inorg. Chem.* **1996**, *35*, 5272.
(7) Kleinke, H.; Franzen, H. F. *J. Alloys Compd.* **1996**, *238*, 68; Kleinke, H.; Franzen, H. F. *J. Alloys Compd.* **1997**, *255*, 110.
(8) Kleinke, H.; Franzen, H. F. *J. Angew. Chem., Int. Ed. Engl.* **1997**, *36*, 513.
(9) Kleinke, H.; Franzen, H. F. *J. Solid State Chem.* **1988**, *137*, 218.
(10) Maggard, P. A.; Corbett, J. D. *Angew. Chem., Int. Ed. Engl.* **1997**, *18*, 336.
(11) Maggard, P. A.; Corbett, J. D. *Inorg. Chem.* **1998**, *37*, 814.
(12) Owens, J. P.; Franzen, H. F. *Acta Crystallogr.* **1994**, *B30*, 427.
(13) Weirich, T. E.; Pöttgen R.; Simon, A. *Z. Kristallogr.* **1996**, *211*, 927.
(14) Corbett, J. D. In *Modern Perspectives in Inorganic Crystal Chemistry*, Parthé, E., Ed.; NATO ASI Series C; Kluwer Academic Publishers: Dordrecht, The Netherlands, 1992; pp 27−56.
(15) Brewer, L.; Wengert, P. R. *Metallurg. Trans.* **1973**, *4*, 2674.

10.1021/ic981073a CCC: $18.00
Published on Web 03/31/1999

Table 1. Some Data Collection and Refinement Parameters for $Sc_5Ni_2Te_2$

formula weight	597.42
space group, Z	*Pnma* (No. 62), 4
lattice parameters[a]	
a (Å)	17.862(1)
b (Å)	3.9533(3)
c (Å)	10.6398(6)
V (Å^3)	751.3(1)
d_{calc}, g/cm^3	5.281
μ, cm^{-1} (Mo Kα)	167.35
R; R_w[b] (%)	3.2, 3.2

[a] Guinier data, Cu Kα, 23 °C, 58 lines. [b] $R = \sum||F_o| - |F_c||/\sum|F_o|$; $R_w = [\sum w(|F_o| - |F_c|)^2/\sum w(F_o)^2]^{1/2}$; $w = \sigma_F^{-2}$.

Experimental Section

All materials were handled in He-filled or N_2-filled gloveboxes to reduce contamination by adventitious impurities. The elements were used as received: Sc turnings, Aldrich 99.7%; Te powder, Aldrich 99.99%; Ni powder, Alfa 99.95%. The synthesis of $Sc_5Ni_2Te_2$ began with the preparation of Sc_2Te_3 as described previously.[10] The Sc_2Te_3, Ni, and Sc to give a 3:1:1 (Sc:Ni:Te) stoichiometry were first loaded into a tantalum tube welded at one end. The other end of the tube was then crimped shut inside the glovebox and transferred to an arc-welder. The tube was sealed after the welder had been evacuated and backfilled with argon. Such containers were then sealed inside evacuated and well-flamed fused silica jackets, heated at 1000 °C for 24 h, cooled to 700 °C at 5 °C/hr, and then allowed to cool in air. Guinier powder diffraction on the product of the first reaction showed what was subsequently found to be $Sc_5Ni_2Te_2$ had been obtained in ≥80% yield, plus ScTe. Further reactions with the indicated 5:2:2 stoichiometry at higher or lower temperatures only yielded a neighboring ternary phase Sc_6NiTe_2[16] or ScTe and ScNi. Also, arc-melting reactions at the 5:2:2 composition did not yield $Sc_5Ni_2Te_2$. However, reactions loaded off-stoichiometry (~Sc_3NiTe) yielded higher quantities of $Sc_5Ni_2Te_2$, evidently because some Ni had been lost into the container in the former reactions. The same synthetic techniques with Fe, Co, and Cu (M) as the late transition metal did not yield any of the analogous $Sc_5M_2Te_2$ phases.

Powder X-ray Diffraction. The powder diffraction patterns of $Sc_5Ni_2Te_2$ were obtained with the aid of an Enraf-Nonius Guinier powder camera and monochromatic Cu Kα_1 radiation. The samples were powdered, mixed with standard silicon (NIST), and placed between two strips of cellophane tape on a frame that mounted on the sample rotation motor. Lattice parameters were obtained with the aid of least-squares refinement of 58 indexed lines with 2θ values calibrated by a nonlinear fit to the positions of the standard Si lines (Table 1).

Single-Crystal Diffraction. Several irregularly shaped, silvery crystals were mounted inside 0.3-mm i.d. glass capillaries that were sealed off and mounted on metal pins. Their quality was checked by means of Laue photographs. A diffraction data set for the best crystal was measured on a Rigaku AFC6R diffractometer (monochromated Mo Kα_1 radiation) at room temperature. Twenty-five centered reflections gathered from a random search were used to determine provisional lattice constants and the crystal system. Two octants of data were collected (h, k, $\pm l$) to $2\Theta_{max} = 60°$ and corrected for Lorentz and polarization effects. The data were further corrected for absorption with the aid of two ψ-scans. Of 4627 measured reflections, 1938 had $I > 3\sigma(I)$ and 653 of these were unique. Extinction conditions and statistical evidence for centricity indicated one possible space group, *Pnma*. The structure was solved by direct methods (SHELXS[17]) and refined with the package TEXSAN[18] in this space group. After isotropic refinement, the data averaged with $R_{av} = 9.2\%$, and the final anisotropic refinement converged at $R(F)/R_w = 3.2/3.2\%$ for the composition $Sc_5Ni_2Te_2$. Some data for these processes are listed in Table 1, and the atomic positions and isotropic-equivalent temperature factors are given in Table 2. Additional data collection and refinement parameters, the anisotropic displacement parameters, and a complete distance list are in the Supporting Information. These as well as the F_o/F_c listing are also available from J.D.C.

Table 2. Positional and Isotropic-Equivalent Thermal Parameters for $Sc_5Ni_2Te_2$

atom	x	z	B_{eq} (Å^2)[b]
Te1	0.10736(6)	0.5103(1)	0.71(4)
Te2	0.73263(6)	0.3098(1)	0.71(4)
Ni1	0.9159(1)	0.1038(2)	0.83(7)
Ni2	0.9939(1)	0.8261(2)	0.84(8)
Sc1	0.1526(2)	0.7819(3)	0.7(1)
Sc2	0.2730(2)	0.4786(3)	0.8(1)
Sc3	0.8663(2)	0.6963(3)	0.8(1)
Sc4	0.5740(2)	0.4410(3)	0.8(1)
Sc5	0.9808(2)	0.3281(3)	0.8(1)

[a] All atoms on m, $y = 1/4$. [b] $B_{eq} = (8\pi^2/3)\sum_i\sum_j U_{ij} a_i^* a_j^* \vec{a}_i \vec{a}_j$.

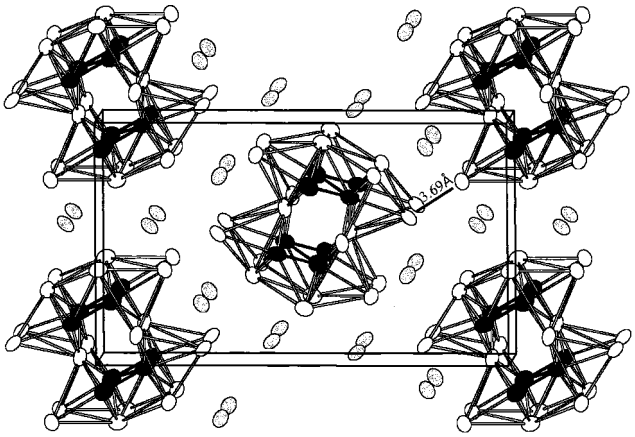

Figure 1. Near-[010] section of the chain structure of $Sc_5Ni_2Te_2$ (99.9% probability ellipsoids). The Ni atoms are black, Sc, white, and Te, gray ellipsoids. The shortest interchain distance is marked. The a axis is horizontal.

Band Calculations. Extended Hückel calculations were carried out within the tight-binding approximation[19] for the full structure of $Sc_5Ni_2Te_2$ at 48 k-points spread out over the irreducible wedge. H_{ii} parameters employed were the values iterated to charge consistency for Sc from Sc_2Te,[10] and for Ni from Sc_6NiTe_2[16] (eV): Sc 4s, −6.75; 4p, −3.38; 3d, −6.12; Ni 4s, −5.58; 4p, −2.41; 3d, −7.82; Te 6s, −21.20; 6p, −12.00. Very similar energies were also obtained for the first two from charge iteration on ScNi (CsCl type). The charge interation for Ni gave much more suitable results for this polar compound than those from density functional theory (−8.13, −4.18, −12.40 eV, respectively[20]).

Results and Discussion

Structural Description. A near-[010] section of the $Sc_5Ni_2Te_2$ structure viewed along the short 3.95 Å axis is given in Figure 1. The atom distribution can be viewed as pairs of extended zigzag chains of nickel (black) that are sheathed by scandium (open) and are in turn well-separated by single tellurium atoms (gray). The shortest distance between separate metal chains, d(Sc2−Sc3) = 3.69 Å (marked), is at best a weak interaction (below). Figure 2 illustrates the repeat unit in one chain along with atom labels and distances that have appreciable overlap populations (vide infra). To help understand the structure, Figure 3 shows a side view of one-half of the composite chain as viewed more or less along [301], Figure 1. The repeat units here are rectangular scandium pyramids [Sc2,

(16) Maggard, P. A.; Corbett, J. D., unpublished.
(17) Sheldrick, M. SHELXS-86. Universität Göttingen, Germany, 1986.
(18) TEXSAN, Version 6.0, Molecular Structure Corp., The Woodlands, Texas, 1990.
(19) Hoffman, R. *J. Chem. Phys.* **1963**, *39*, 1397; Whangbo, M.; Hoffman, R. *J. Am. Chem. Soc.* **1978**, *100*, 6093.
(20) Vela, A.; Gázquez, J. L. *J. Phys. Chem.* **1988**, *92*, 5688.

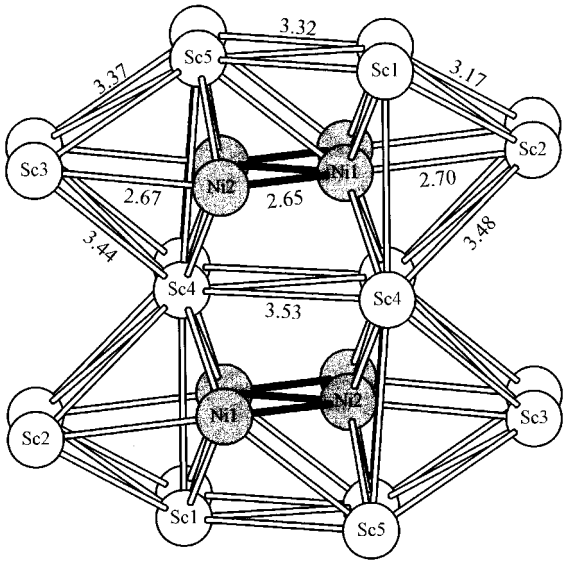

Figure 2. The centrosymmetric repeat unit in the Sc_5Ni_2 chain, with the numbering scheme and independent distances marked. Nickel atoms and Ni−Ni bonds are darker.

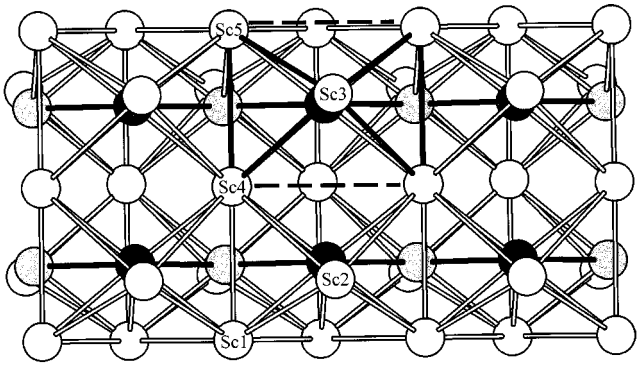

Figure 3. Side view of one-half of the Sc_5Ni_2 metal chain (Figure 2), with the short $b = 3.95$ Å repeat horizontal. The Ni atoms are darkened with the gray one further away. Note the construction of Ni-based rectangular pyramids of Sc; one is marked by a heavier outline.

Sc1 (×2), Sc4 (×2) and Sc3, Sc4 (×2), Sc5 (×2)] (one is highlighted) that share Sc4−Sc4 edges in pairs and Sc1−Sc4−Sc5 edges infinitely along $\vec{b}$. Each rectangular pyramid has a nickel atom 0.54 Å outside of the base. Two of these composites are then assembled base-to-base with a relative displacement of $b/2$ to generate the full chains seen in Figures 1 and 2. This assembly generates additional Sc1−Sc5 (top and bottom) and Sc4−Sc4 bonds across Figure 1 plus the pair of parallel zigzag chains of nickel that run down the central channel of the chain. The Ni−Ni distance within the zigzag chains is 2.66 Å (the single bond distance is given as 2.31 Å[21]) whereas the closest separation between the eclipsed Ni chains is 3.27 Å. The scandium atoms about the two nickel strings exhibit Sc−Ni distances over 2.62−2.87 Å, whereas Sc−Sc distances around the outside of the chain span 3.17−3.48 Å.

Numerous older structures have demonstrated that a preferred environment for the late transition metal is in the center of a multicapped trigonal prism of the early transition metal.[2−8] In the present structure, four such chains of nickel centered within confacial scandium trigonal prisms can be viewed as having been condensed together, but the relationship is not as clear and direct. One such Sc2-capped member in the upper right of Figure 2 consists of Sc1 (×2) and Sc4 (×2) as two of the side edges, with the third edge Ni2−Ni1 pair which also centers the next interpenetrating trigonal prism. The 2:5 ratio of nickel to scandium, relative to that in Sc_6NiTe_2,[14] predicates such condensation. Another description of this one-dimensional array is in terms of zigzag chains. If the Sc−Ni connectivity of the structure is neglected for the moment, it can be seen in Figure 2 that the outside shell of the chain is composed entirely of zigzag Sc−Sc chains along $\vec{b}$ that share vertexes, the comparable Ni−Ni chains being added internally. Although the later interpretation is not the most useful in terms of understanding the local bonding, it is visually helpful.

Table 3. Selected Metal−Metal Distances (Å) and Overlap Populations in $Sc_5Ni_2Te_2$

atom 1	atom 2	distance		overlap pop. per pair
Sc1	Sc2	3.17	×2	0.199
Sc1	Sc4	3.27		0.194
Sc4	Sc5	3.31	×2	0.172
Sc2	Sc4	3.48	×2	0.102
Sc3	Sc4	3.44	×2	0.108
Sc3	Sc5	3.38	×2	0.099
Sc1	Sc5	3.32	×2	0.093
Sc4	Sc4	3.53	×2	0.082
Sc2	Sc2	3.95[a]	×2	0.045
Sc4	Sc4	3.95[a]	×2	0.037
Sc2	Sc3	3.69[b]		0.036
Sc1	Sc3	3.83[b]	×2	0.028
Sc1	Sc2	3.88[b]	×2	0.018
Sc1	Sc1	3.95[a]	×2	0.015
Sc5	Sc5	3.95[a]	×2	0.009
Ni1	Ni2	2.66	×2	0.020
Ni1	Ni2	3.27[c]		−0.007
Ni2	Sc3	2.67		0.209
Ni2	Sc4	2.62	×2	0.191
Ni2	Sc5	2.61	×2	0.192
Ni1	Sc1	2.62	×2	0.184
Ni1	Sc4	2.64	×2	0.178
Ni1	Sc2	2.70		0.174
Ni1	Sc5	2.65		0.174
Ni2	Sc4	2.86		0.107
Ni1	Sc4	2.86		0.104
Ni2	Sc1	2.87		0.098

[a] Unit cell repeat in the chain. [b] Interchain distance. [c] Shortest distance between two nickel chains.

The description of all of the pairwise atom−atom distances within the Sc_5Ni_2 chain is fairly involved. Some of these are marked in Figure 2, and they are also listed in order of decreasing pairwise overlap populations in Table 3. (The complete distance listing is given in the Supporting Information.) It should be noted that the chain is centrosymmetric and only one-half of the interactions need to be considered. While Sc1 is bonded twice to Ni1 (2.62 Å) and once to Ni2 (2.87 Å, across the double Ni chain), Sc5 is connected in parallel but more tightly, twice to Ni2 (2.61 Å) and once to Ni1 (2.65 Å). Sc1 and Sc5 also form a zigzag pattern atop the double nickel chains with Sc1−Sc5 = 3.32 Å (×2). Internally, Sc4 occupies a special position more inside of the chain, and the farthest from any tellurium atom. The Sc4 has two short contacts to each of Ni1 and Ni2, 2.64 and 2.62 Å, respectively, and long diagonals across the chain center to both Ni (2.86 Å). Interestingly, there are also short distances between Sc4 and both Sc1 and Sc5, edges in the square pyramids (3.27 and 3.31 Å), perhaps because of their common nickel neighbors. Finally, the comparable Sc2 and Sc3 atoms, the apexes of the rectangular pyramids described earlier, are also bonded to their basal Ni1 (2.70 Å) and Ni2 (2.67 Å), respectively, and also twice each to Sc4 and Sc1 or Sc5 at 3.17−3.48 Å. The two opposed double chains of

(21) Pauling, L. *The Nature of the Chemical Bond*; Cornell University Press: Ithaca, NY, 1960; p 400.

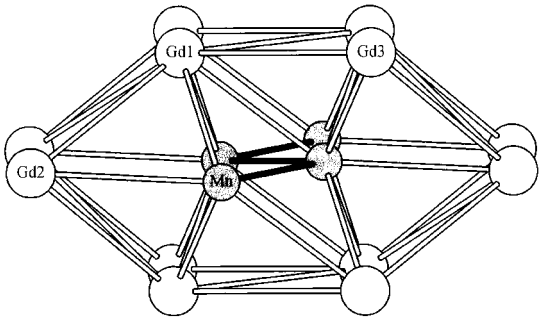

Figure 4. A [010] view of the metal chain in Gd_3MnI_3[22] along the short repeat. Compare with the top or bottom half of the Sc_5Ni_2 chain in Figure 3.

rectangular pyramids, $Sc_2(Sc_{6/2})Ni_2$, left and right in Figure 2, are then interconnected through Sc1−Sc5, Sc4−Sc4, and Ni1−Ni2 bonding. (This description is helpful later in understanding the overlap populations.) The nonequivalent nickel atoms are reflected in the unequal but generally similar distances about them, the most disparate of which being Ni1−Sc5, 2.65 Å and Ni2−Sc1, 2.87 Å (not drawn) which reflect the skewness of the centrosymmetric chain. Fourier difference maps do not show any extra electron density in the central channel of the chain. The chains are not significantly interbonded, as will be shown for the shortest separation of this kind marked in Figure 1, 3.69 Å for Sc2···Sc3. The Te−Te distances are all ≥3.95 Å. These structural motifs and atomic distances support the 1D chain assignment to $Sc_5Ni_2Te_2$.

Remarkably similar structural characteristics are found in the chains in Gd_3MnI_3,[22] the $(Gd_3Mn)_2$ portion of which is shown along the short 4.13 Å axis in Figure 4.[23] This is very similar to the upper or lower half of the Sc_5Ni_2 chain (Figures 2,3). The iodide was likewise described as the base-to-base assembly of two chains of trans-edge-sharing rectangular pyramids, which is a very atypical halide structure. This has been classified as a distortion extreme of a family of compounds originating with $Pr_3(Ru)I_3$, viz., double chains of *Z*-centered R_6 octahedra that share trans edges and are further condensed side-by-side. Their progressive distortions in other examples can be described as the partial fusion of the recognizable twin octahedral chains in Pr_3I_3Ru, etc., as two adjoining octahedra begin to merge and the *Z* elements approach one another.[24] Although the $Sc_5Ni_2Te_2$ and Gd_3MnI_3 compositions and geometries may be readily interrelated, the electron-poorer interstitial Mn also exhibits significant Mn−Mn bonding.

Theoretical Calculations. Intuitively, the character of the bonding in $Sc_5Ni_2Te_2$ must be highly delocalized, the bonded metal neighbors ranging from five about Sc2 and Sc3 through eight for Sc1 and Sc5, 10 for each Ni, and 14 for Sc4. Band calculations seemed necessary to clarify the situation. Figure 5 shows the total DOS for $Sc_5Ni_2Te_2$. Typical for these relatively electron-poor compounds, the Fermi level resides on the low-energy side of a prominent conduction band composed of about 90% scandium d and s orbitals and 10% nickel contributions. The nickel d (and Sc d) states comprise all of the lower valence bands between ∼−8.5 and −7.0 eV, with tellurium states being the majority at still lower energies (off scale). A near gap at ∼−6.9 eV occurs with 36 of the 47 total electrons per formula unit. The band below there can be described simply, but not

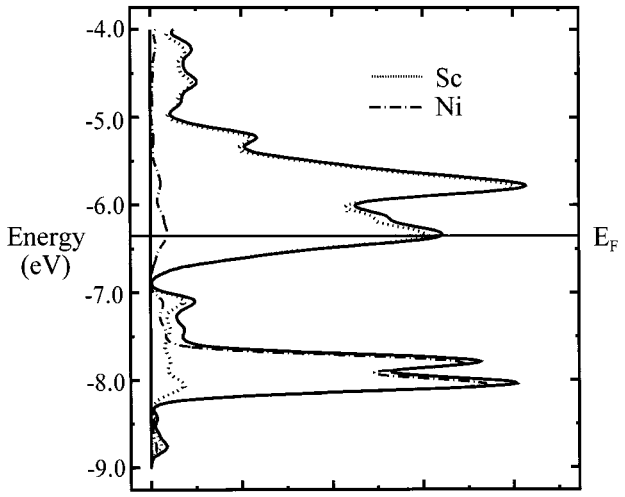

Figure 5. The densities-of-states from the EHTB band calculation for $Sc_5Ni_2Te_2$. The separate Sc and Ni contributions are projected out.

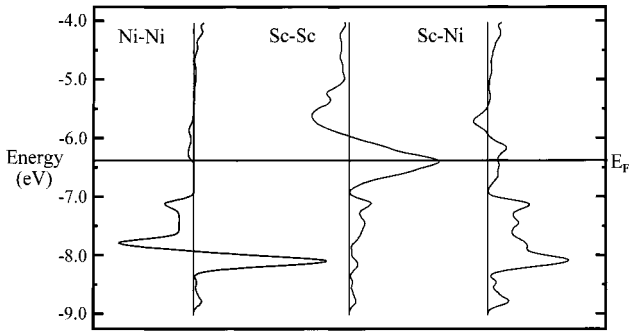

Figure 6. Total COOP (overlap-weighted orbital population) curves for indicated pairwise interactions in $Sc_5Ni_2Te_2$.

rigorously, as 2 Ni (d^{10}) and 2 Te (s^2p^6), with the 11 electrons left over in the conduction band.

Figure 6 shows the COOP curves for total Ni−Ni, Sc−Sc, and Sc−Ni bonding. E_F falls largely within bonding regions for both Sc−Sc and Sc−Ni and 0.4 eV below the onset of Sc−Sc antibonding states. On the other hand, the Fermi level falls in a nonbonding region for Ni−Ni interactions, these being virtually closed shell above ∼−7.0 eV. This is a common behavior for M−M bonding of late transition metals as they achieve a closed shell d^{10} configuration, as noted in La_2Ni_2I.[25] Other cases of early-late transition metal chalcogenide structures have been observed to optimize the M−Ni bonding as revealed by COOP curves.[4] It is interesting that this is not the situation here, albeit in a structure that does not involve the trigonal prisms in a linear face-sharing motif as before.

A complex structure such as this presents an ample variety of distances and bond strengths. Comparisons of bond distances with overlap populations allow one to ascertain where matrix effects, separations fixed more by geometric relationships, may be more important than bonding in near-neighbor contacts. For this purpose, pairwise overlap populations for Sc−Sc, Sc−Ni, and Ni−Ni are listed in Table 3 in decreasing magnitude along with the corresponding distances. These change in parallel fairly well, but there are some significant deviations that assist in highlighting important bonding details. For one, the Sc1−Sc5 bridging interactions at 3.32 Å lie fairly low in the list (0.093). The natural assumption is that this distance is moderately to heavily influenced by matrix effects, in concert with the

(22) Ebihara, M.; Martin, J. D.; Corbett, J. D. *Inorg. Chem.* **1994**, *33*, 2078.
(23) This relationship was pointed out to us by a perceptive reviewer.
(24) Payne, M. W.; Dorhout, P. K.; Kim, S.-J.; Hughbanks, T. R.; Corbett, J. D. *Inorg. Chem.* **1992**, *32*, 1389.
(25) Hong, S.-T.; Martin, J. D.; Corbett, J. D. *Inorg. Chem.* **1998**, *37*, 3385.

suggestion made earlier that the structure could be described as two edge-sharing sheets built from square pyramids and "glued" together by Ni−Sc (and Ni−Ni) bonding, Figure 2. The other cross-distance, Sc4−Sc4, is longer but more central, and it has only a slightly lower population, 0.082 at 3.53 Å. The Sc and Ni orbital energies are close enough that they do mix well and give substantial overlap populations, whereas this is not true for the Ni−Ni bonding when the atoms are this well-reduced and have virtually closed shells. In this case, the observed distance in the zigzag chain, which corresponds to a Pauling bond order of 0.26, is quite misleading regarding the actual bonding magnitude.

Other noteworthy differences are the relatively large overlaps for Sc2−Sc2 (0.045) and Sc4−Sc4 (0.037) (but not for Sc1−Sc1, Sc3−Sc3, and Sc5−Sc5) along the 3.95 Å chain repeat. This result is not surprising for Sc4, which resides centrally within the chain and shows effects that parallel those noted for Sc_2Te and Sc_8Te_3 where electrons appear to be concentrated within metal-rich cluster chains that are isolated by nonmetals neighbors.[9,10] But strong bonding along the chain for Sc2 as well seems unusual as these atoms reside more on the periphery of the chains, with three tellurium near neighbors. The larger population here may mean additional bonding takes place for scandium that otherwise has fewer (five) near metal neighbors. Scandium 3 has the largest number of close Te neighbors (4) and thence little Sc3−Sc3 bonding.

The interchain Sc−Sc distances lie near the bottom of the overlap population list. The shortest distance between the chains (Sc2−Sc3, 3.69 Å) has an overlap population of 0.036, followed by smaller values for analogous but longer distances (Sc1−Sc3, 0.028; Sc1−Sc2, 0.018). There are evidently only meager amounts of electron density between the chains (<∼15% of the larger internal populations), but whether these are remarkable or substantial is doubtful.

The notion was posited before that Sc−Ni bonding holds the chain together, an idea that goes back to the original studies of early-late transition metal bonding by Brewer and Wengert.[15] These overlaps are given at the bottom of Table 3. The seven shorter types of Sc−Ni contacts around 2.61−2.70 Å have overlap populations of about 0.17 to 0.21, while the three longer contacts of 2.86 Å involving Sc4 or a long diagonal to Sc1 have lower values, ∼0.10. One important detail is that the Ni2−Sc3 distance to the apex of one rectangular pyramid has a somewhat larger overlap population than for the analogous Ni1−Sc2 (0.209 vs 0.174), in parallel with the generally different distances about these two-pseudo-equivalent atoms (i.e., Sc2−Sc1 vs Sc3−Sc5). Similarly the "equivalent" Sc1−Ni2 and Sc5−Ni1 diagonals differ by 0.22 Å and in parallel, so do the overlap populations. The causes of these distortions are complex and perhaps tied up with the factors behind optimization of overall bonding.

Structural Comparisons. $Sc_5Ni_2Te_2$ is nominally isotypic with $Hf_5Co_{1+x}P_{3-x}$, but there are in detail many differences in the bonding. These involve the ordering pattern, the sizes of the nonmetals and the transition metals, and presumably, the electron counts. Figure 7 shows the $Hf_5Co_{1+x}P_{3-x}$ structure[7] nearly along [010], with the bonds in the double zigzag chain unit that are comparable to those in Figure 1 outlined in black, and the additional metal−metal interactions about it as open bonds. The Hf−Hf and Hf−Co bonding in this occurs in essentially a 3D arrangement, as judged by distances and, especially, overlap populations.[7] The few Hf−Hf distances displayed on the structure show that the equivalent "interchain" distances are approximately equal to or less than those within.

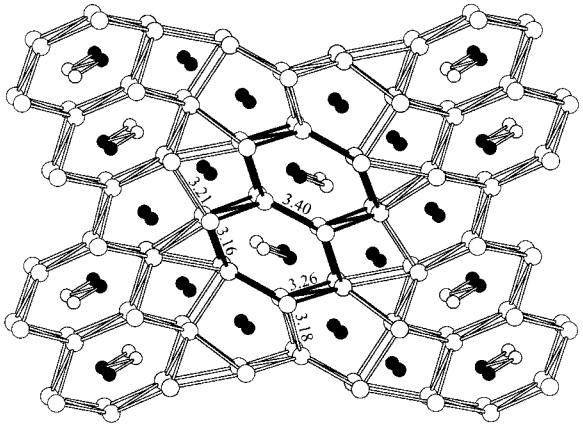

Figure 7. Near-[010] projection of the structure of $Hf_5Co_{1+x}P_{3-x}$ ($0 \leq x \leq 0.5$) with Co gray, P black.[7] The chain unit evident in $Sc_5Ni_2Te_2$ (Figure 1) is outlined.

This condensation of the building units expresses the greater number of metal-based electrons for hafnium compared with scandium and, most certainly, the smaller size of phosphorus compared with tellurium. Once again, as was the case for the M_8Ch_3 phases (M = Sc, Y; Ch = Se, Te vs Te_8Ch_3, Ch = S, Se),[9] there is a cooperative effect of increased anion size and decreased valence electron concentration that acts to reduce the dimensionality of the scandium interactions.

In addition to the reduction in dimensionality in $Sc_5Ni_2Te_2$, there is also a substantial difference in ordering of the nonmetal and transition metal atoms. In $Hf_5Co_{1+x}P_{3-x}$,[7] a phase width ($0 \leq x \leq 0.5$) arises from the varying occupancy of one intrachain position by cobalt (gray) and phosphorus (black). The authors attributed this in part to the similar atomic sizes and their distances to hafnium. For $Sc_5Ni_2Te_2$, the intrachain zigzag chains are composed solely of nickel atoms, and the interchain cavities are filled only by tellurium, which emphasize the lowered dimensionality. This new ordering rests with the fact that tellurium and nickel have disparate atomic sizes and very different distances to scandium. Furthermore, a large phase width is no longer a structural feature. The resultant ordering still generates only fairly weak Ni−Ni bonding. The variability between these structures is remarkable.

There are interesting parallels and contrasts between the metal-rich chalcogenide compounds of the rare-earth elements (R) and the longer known halides. Twice as many halogen as chalcogen atoms would be needed to achieve the same electron count per metal, and this anion preponderance alone would produce better separation of the metal-bonded units and reduction of the dimensionality of the halides, as observed. Isolated halide clusters are thus much more common, and chains of edge-sharing metal octahedra are relatively fewer (Y_2Cl_3, Sc_5Cl_8C, Y_4I_5C, etc.). The halides are, in fact, generally so electron-poor that interstitial heteroatoms are nearly always required for stability. Including the electron count of the interstitial gives 2.3−2.8 electrons per cluster metal, 2.8−3.2 e^- in chains, and X/R values of roughly 1.0 (condensed clusters) to 2.0 (isolated).[14] (The odd binary Y_2Cl_3 and Sc_7Cl_{10} remain exceptions at 1.8 e^-/R.) The binary chalcogenides Sc_2Te and Sc_8Te_3 achieve only slightly lower electron counts than cluster halides, 2.0−2.25 per metal, but with disproportionately lower Ch/R values, 0.5−0.38. In other words, the grossest analysis suggests that both classes of the metal-richest group 3 compounds achieve similar electron counts per metal, ca. 2.0−2.5, but at greatly

different stoichiometries: 1.3−1.7 X/R vs ≤ 0.5 Ch/R.[26] The latter nicely correlates with the notably greater aggregation found in the metal-richest chalcogenides. As with later transition metal chalcogenides, these too would appear to be driven by M−M bonding when the anion number is insufficient to give good sheathing of the metal aggregate. It's harder to compare these two families of compounds electronically when they contain late transition metal components (Gd_3MnI_3 vs $Sc_5Ni_2Te_2$), but if we ignore the contributions of the latter the difference in VEC is similarly low (2.0 vs 2.2).

Finally, the roles of the anions are rather different, evidently because of differences in their quantity. Halides (Cl, Br, I) generally exhibit several very discrete functions on these clusters or chains, being two to four coordinate as they bridge all exposed edges and bond exo at all vertexes of the cluster units. Exceptions are rare.[14] The greatly reduced telluride numbers lead to much higher coordination numbers and less regular geometries, usually some form of an augmented trigonal prism. In the present compound, two different tellurides each have 6−7 neighbors at 2.91−3.06 Å, plus two more contacts at 3.16 Å. These marked differences have generally led us to include the halides in illustrations but to omit the less specific chalcogenide environments. One would in fact expect the chalcogenide−metal interactions to be somewhat more covalent.

Conclusions. $Sc_5Ni_2Te_2$ is significant because it represents the first extension of early-late transition metal bonding in chalcogenides to the earliest, and most electron-impoverished transition metals. The structure is built up from double nickel zigzag chains sheathered by scandium atoms and separated from other Sc_5Ni_2 chains by tellurium atoms. The metal substructure can be envisaged as trans-edge-shared double square pyramid chains "glued" together at their bases mainly by Sc−Ni bonding. Reduction in dimensionality compared with $Hf_5Co_{1+x}P_{3-x}$ results from a new ordering of the nonmetal and late transition metal and the different anionic nature of tellurium. A decreased number of metal-based electrons is in concert with the absence of interchain bonds via tellurium in this new phase. These structural interrelationships aid in the understanding of this new ternary phase.

Acknowledgment. This work was supported by the National Science Foundation, Solid State Chemistry, via grants DMR-9510278 and -9809850 and was carried out in the facilities of the Ames Laboratory, U.S. Department of Energy.

Supporting Information Available: Tables of additional crystallographic and refinement parameters, anisotropic thermal parameters, and a complete listing of nearest-neighbor distances (PDF). This material is available free of charge via the Internet at http://pubs.acs.org.

IC981073A

(26) The lowest X/R in individual closed-shell clusters is about 1.7 [Sc-($Sc_6Cl_{12}N$), $Y_6I_{10}Os$]. Oxidation to give larger X/R values and less interbridged cluster arrays, up to X/R = 3 (R_6X_{18}), are compensated by incorporation of electron-richer Z or additional alkali metals, or both, the e^-/R remaining close to 2.3 throughout.